



**HAL**  
open science

## Intermodulation Products of a CMOS SP6T Antenna Switch: Results Comparison Between an Experimental Test-Bench and a Corresponding Simulated Virtual Test-Bench

M. Ben-Sassi, H. Saleh, O. Sow, I. Lahbib, Greg U'Ren, C. Hellepee, D. Passerieux, G. Neveux, Denis Barataud

### ► To cite this version:

M. Ben-Sassi, H. Saleh, O. Sow, I. Lahbib, Greg U'Ren, et al.. Intermodulation Products of a CMOS SP6T Antenna Switch: Results Comparison Between an Experimental Test-Bench and a Corresponding Simulated Virtual Test-Bench. 2021 16th European Microwave Integrated Circuits Conference (EuMIC), Apr 2022, London, France. pp.9-12, 10.23919/EuMIC50153.2022.9783860 . hal-04489976

**HAL Id: hal-04489976**

**<https://unilim.hal.science/hal-04489976>**

Submitted on 7 Mar 2024

**HAL** is a multi-disciplinary open access archive for the deposit and dissemination of scientific research documents, whether they are published or not. The documents may come from teaching and research institutions in France or abroad, or from public or private research centers.

L'archive ouverte pluridisciplinaire **HAL**, est destinée au dépôt et à la diffusion de documents scientifiques de niveau recherche, publiés ou non, émanant des établissements d'enseignement et de recherche français ou étrangers, des laboratoires publics ou privés.

# Intermodulation Products of a CMOS SP6T Antenna Switch: Results Comparison Between an Experimental Test-Bench and a Corresponding Simulated Virtual Test-Bench

M. Ben-Sassi<sup>#1</sup>, H. Saleh<sup>#2</sup>, O. Sow<sup>#3</sup>, I. Lahbib<sup>#4</sup> and Greg D.U'Ren<sup>#5</sup>  
 C. Hellepee<sup>\*1</sup>, D. Passerieux<sup>\*2</sup>, G. Neveux<sup>\*3</sup> and D. Barataud<sup>\*4</sup>

<sup>#</sup>X-FAB France, Corbeil-Essonnes, <sup>\*</sup>XLIM-UMR CNRS n°: 7252, University of Limoges, France

<sup>#</sup>Marwen.Ben-Sassi@xfab.com

**Abstract** — This paper presents a comparison between Third Order Intermodulation Distortion (IMD3) measurements and simulations of a RF-SOI SP6T antenna switch. The originality of the paper lies in the development of a simulation tool representing a virtual test-bench corresponding to the experimental set-up used for the measurements of Intermodulation products. All the passive devices (circulators, isolators and filters) used in the experimental test-bench have been characterized in terms of [S] parameters. These [S] matrices have been then implemented into the software environment to simulate the experimental test-bench. A non-linear behavioral model of the SP6T switch from X-Fab foundry has been extracted, validated and implemented in the virtual test-bench. Two-tone Harmonic Balance simulations are performed with this behavioral model. The measured and simulated IMD3 results are finally compared.

**Keywords** — IMD3, Two-tone HB Simulation, SP6T Switch

## I. INTRODUCTION

Needs for higher data rates in new mobile communication generations are continuously growing. Recently launched 4G TLE-A smartphones can support data rates up to 1 Gbps. These features are driven by the development of revolutionary telecommunication standards and complex front-end architectures such as Multiple Input Multiple Output (MIMO) and Carrier Aggregation (CA). CA allows simultaneous transmission on multiple frequency bands to increase data rates. It is employed in 4G and is expected to grow up in the 5G with the higher number of available frequency bands. A main component in a RF Front-End Module (FEM) of a User Equipment (UE) featuring CA is the antenna switch that selects which transmitter (Tx) or receiver (Rx) path can be connected to the antenna. Therefore, many transmission signals with different frequencies are present at the antenna vicinity and pass through the switch toward their receiver destination. Due to the use of multiple bands simultaneously for uplink and downlink CA, unwanted Inter-Modulation Distortion (IMD) products are generated and could interfere with wanted signals. If the linearity of the antenna switch that is simultaneously processing the Tx, Rx and interferer blocking signals is not high enough, the IMD products of the blocker signal and the Tx signal may fall on the own Rx band. For the IMD products not to cause performance degradation for the receiver, their power levels should not exceed the reference sensitivity power level [3]: the ability of a receiver

to receive a wanted signal at its assigned channel frequency in the presence of an unwanted interferer. With the increased number of frequencies in 4G and 5G, interferences and consequently IMD products are more likely to happen. IMD products characterization and modelling of antenna switches is crucial to help designers adopt adequate semiconductor technologies and best linearity architecture for FEM systems.

From practical point of view, RF switches IMD products measurement is challenging due to their low power levels. 3GPP technical specification set receivers' reference sensitivity power level for the different bands between -90 dBm and -100 dBm. Switches' IMD products should not exceed this reference level for receiver performance not to be degraded. Measurement of IMD product levels below -100 dBm requires high linearity test components and very high sensitivity for receiver instruments.

This work aims to numerically reproduce third-order IMD phenomenon in antenna switches. It provides designers with a useful tool that reproduces measurement and can be easily implemented. The proposed approach relies on the development of a behavioral model for the switch linearity and the comparison to measurement. The experimental setup is similar to the one proposed in [1]. The used switch is a SP6T made with a CMOS RF-SOI technology and operates in the cellular band [0.4 GHz – 2.7 GHz]. The IMD simulation and measurement are investigated for Tx signal at 1.74 GHz and a jammer (blocking) signal at 1.65 GHz.

## II. BEHAVIORAL RF SWITCH MODEL

A behavioral switch model based on a mathematical equation is defined, as shown in Fig. 1, and used within the virtual test-bench. This model reproduces the transmission behavior between 3 ports of the SP6T but it can easily be expanded to the 6 ports.

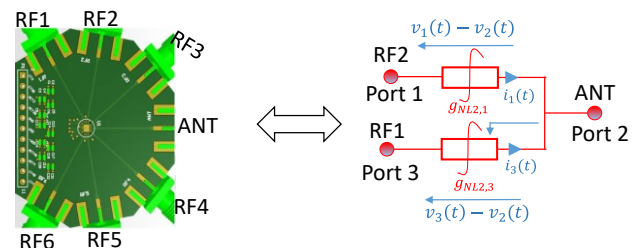


Fig. 1. SP6T switch and its behavioral model

It is based on the use of a modified hyperbolic tangent equation to converge with the real operating mode of the switch. The behavioral model is composed of three RF ports which are connected to Antenna (port 2), to RF2 (port1) and RF1 (port 3). It is based on the use of the mathematical description of two non-linear transconductances  $g_{NL1,2}$  and  $g_{NL2,3}$ , as shown in equations 1 and 2.

$$g_{NL1,2}(t) = \frac{i_1(t)}{v_1(t) - v_2(t)} \quad (1)$$

$$g_{NL2,3}(t) = \frac{i_3(t)}{v_3(t) - v_2(t)} \quad (2)$$

With:

$$i_1(t) = I_1 \tanh(\beta + \alpha[v_1(t) - v_2(t)])[(1 + V_{1leakage}) - V_4] \quad (3)$$

$$\text{and } i_3(t) = I_3 \tanh(\beta + \alpha[v_3(t) - v_2(t)])[1 + V_4] \quad (4)$$

- $g_{NLi,j}$ : Non-Linear Transconductance
- $V_{1leakage}$ : Isolation parameter (Real number)
- $V_4$ : Command voltage (Real number)
- $I_1, I_3, \alpha, \beta$ : Real parameters of non linearities
- $v_i(t)$ : voltage at port  $i$

$g_{NL1,2}$  and  $g_{NL2,3}$  represent the two transconductances implemented from antenna to RF1 and antenna to RF2 respectively.

Table 1 presents the different parameters used in the behavioral model equations. The parameters have been extracted from [S] parameter measurements and from large signal CW power measurements at frequencies of interest presented in Fig. 2.

Table 1. RF switch model parameters

Parameter	Value
$V_{1leakage}$	7e-5 V
$\alpha$	0.03
$g_0$	70
$\beta$	0.05
$I_1$	-17.5
$I_3$	2.31

$I_1, I_3, \alpha$  and  $\beta$  are added as real parameters allowing better transmission description for the switch model. The isolation between port (1) and port (2) has been defined within the model using the  $V_{1leakage}$  parameter. A DC command ( $V_4$ ) has been implemented in order to control the transmission configuration of the switch from RF1 to antenna and from RF2 to antenna. In this work, only the signal transmission from antenna to RF1 is taken into account. The DC voltage ( $V_4$ ) is equal to 1 V. For this condition ( $V_4=1$  V),  $g_{NL1,2}$  tends to 0 while  $g_{NL2,3}$  tends to infinity.

Fig. 2 presents the comparison between CW power measurement (RF1 activated) and simulation ( $V_4=1$  V) results at fundamental (H0), 2<sup>nd</sup> (H2) and 3<sup>rd</sup> (H3) harmonic frequencies at 0.9 GHz, 1.8 GHz and 2.7 GHz respectively. A good agreement between CW power measurements and simulation is obtained.

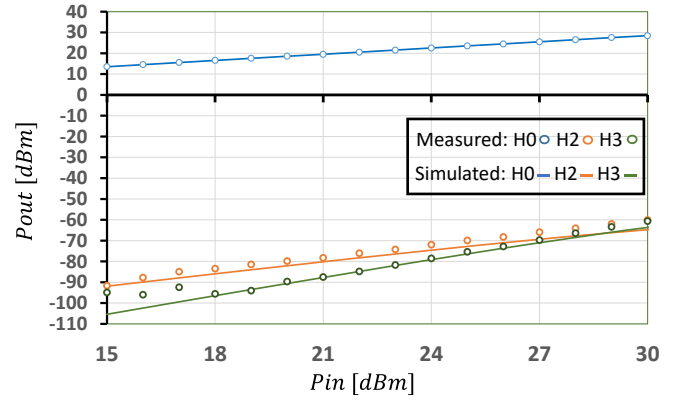


Fig. 2. Comparison of measured and simulated Harmonic distortion results of the model for a 0.9 GHz input fundamental

DC simulation is performed to plot the  $g_{NL2,3}$  non-linearity function and to validate the behavioral model of this transconductance.

Fig. 3 presents the output current  $i_3(t)$  of the  $g_{NL2,3}$  non-linear transconductance versus the voltage difference  $v_3(t) - v_2(t)$ .

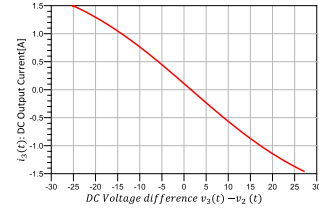


Fig. 3. DC simulation result of the  $g_{NL2,3}(t)$  non-linearity

The  $g_{NL2,3}(t)$  is a weak non-linear function with an offset from the origin.

Fig. 4 presents a comparison between the measured and the simulated  $S_{32}$  parameters of the switch.

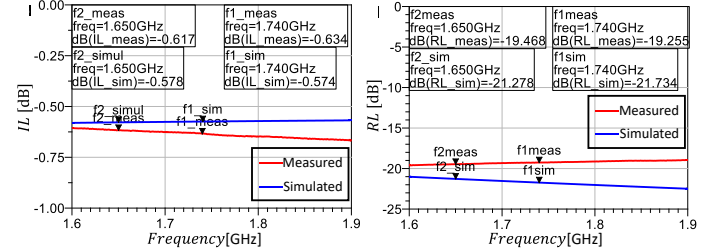


Fig. 4. Comparison of measured and simulated s-parameters of the model

The modelling was focused on  $S_{32}$  transmission behavior.  $S_{22}$  and  $S_{33}$  are matched to 50  $\Omega$ . A good agreement between the measured and the simulated insertion loss ( $S_{32}$ ) is observed. The simulated return loss ( $S_{22}$ ) at the Tx frequency  $f_1 = 1.74$  GHz is also close to the measured one.

### III. PRESENTATION OF THE IMD3 TEST-BENCH

Fig. 5 describes the fundamental architecture of the IMD3 experimental measurement system. Two synchronized RF generators drive the SP6T switch with two RF signals to excite its non-linearities and to measure its potential resulting IMD3. A transmission large signal at the throw port (RF1) and

a jammer (blocking) small signal at the antenna port are exciting the SP6T. The RF path to the throw port, at which the transmission is made, is set to ON state to enable the transmission, where the 5 other paths (RF2 to RF6) are in OFF state and  $50\ \Omega$  loaded.

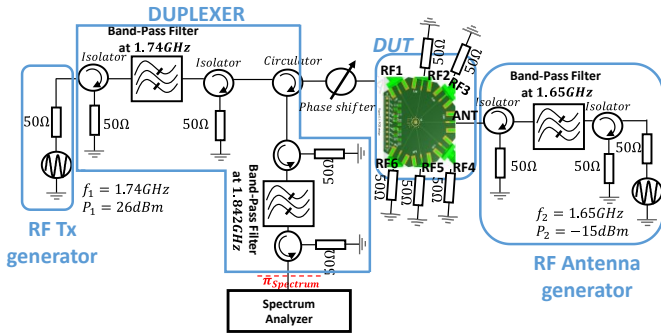


Fig. 5. Block diagram of the IMD3 test-bench with the SP6T configuration

A duplexer is used in this IMD3 test-bench to clearly separate the Rx signal from the Tx signal [1], [2]. It is designed using different band-pass filters associated to  $50\ \Omega$  matched isolators. The duplexer behavior is described later.

The switch is simultaneously driven with a 1.65 GHz ( $f_2$ ) jammer signal with a low power (-15 dBm) at the antenna port, and with a 1.74 GHz ( $f_1$ ) transmission signal with a high power (26 dBm). IMD3 frequency components are measured with a spectrum analyzer which is directly connected to the Rx port of the duplexer.

Table 2 shows the two fundamental frequencies with their associated IMD3 components. The main challenge of the IMD3 characterization is to measure the absolute power levels at the two IMD3 components  $f_3$  and  $f_4$ .

Table 2. Presentation of frequencies of interest used in the IMD3 characterization

IMD3 and fundamental frequencies (GHz)		
$f_1$	$f_{Tx}$	1.74
$f_2$	$f_{jammer}$	1.65
$f_3$	$2 \times f_{Tx} - f_{jammer}$	1.842
$f_4$	$2 \times f_{jammer} - f_{Tx}$	1.55

#### A. Presentation of the duplexer

The main architecture of the duplexer is presented in Fig. 6 (a) [1], [2]. The main challenge for the duplexer is to ensure a very high isolation between port (1) and port (3) to avoid direct leakage from transmission to reception paths.

Isolation between port (1) and port (3) paths is ensured by the use of the band-pass filters at 1.842 GHz and 1.74 GHz. The circulator used in the duplexer allows the transmissions of the signal from port (1) to the port (2) of the duplexer and also the one from the port (2) to the port (3) of the duplexer.

Duplexer is composed of three principal devices. The first one is a [1 GHz- 2 GHz] circulator with 20 dB of isolation. The second one is a band-pass filter centered at  $f_1$  with 70 MHz bandwidth. The third one is a band-pass filter centered at  $f_3$  with 70 MHz bandwidth. It enables the Tx

frequency  $f_1$  at port (1) of the duplexer to be driven to the switch. On the other hand, the incoming signal from the DUT port at the jammer frequency ( $f_2$ ) is driven to the port (3) of the duplexer. That is connected to the receiver.

The signals at  $f_3$  and  $f_4$  are the IMD3 produced in the switch, due to its non-linearity, resulting from the intermodulation between  $f_1$  and  $f_2$  frequencies. The four frequencies  $f_1, f_2, f_3$  and  $f_4$  are driven from the switch to the port (3) through the circulator. The band-pass filter centered at 1.842 GHz selects the  $f_3$  IMD3 frequency component while the  $f_4$  is filtered-out.  $f_3$  is then forwarded to the spectrum analyzer connected to the port (3) of the duplexer. Fig. 6 (b) shows the measured s-parameters of the duplexer.

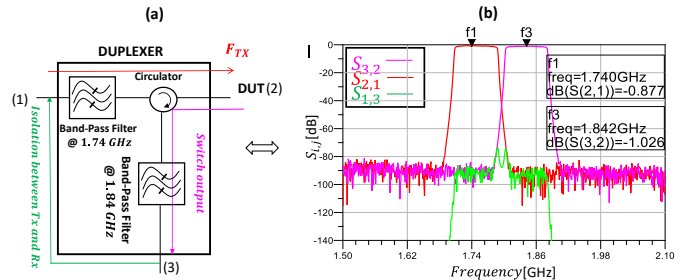


Fig. 6. (a): Block diagram of the duplexer, (b):  $S_{3,2}$ ,  $S_{2,1}$  and  $S_{1,3}$  measurement results of the duplexer

The band-pass filter centered at 1.842 GHz ( $S_{32}$ ) allows filtering the  $f_1$  and  $f_2$  components without too much attenuating the IMD3  $f_3$  frequency component.

The power levels at the two fundamental frequencies  $f_1$  and  $f_2$  are then attenuated to optimize the dynamic range utilization of the spectrum analyzer and avoid compression due to the power levels of  $f_1$  and  $f_2$  signals.

A power calibration between port (2) and port (3) is performed, with reference power sensors at each frequency of interest ( $f_1, f_2$  and  $f_3$ ).

#### IV. COMPARISON BETWEEN MEASUREMENTS RESULTS FROM THE EXPERIMENTAL TEST-BENCH AND SIMULATIONS RESULTS OF THE CORRESPONDING VIRTUAL TEST-BENCH

The proposed configuration of the virtual IMD3 test-bench (2-tone HB simulation) is realized with Keysight ADS<sup>®</sup> software, shown in Fig. 7.

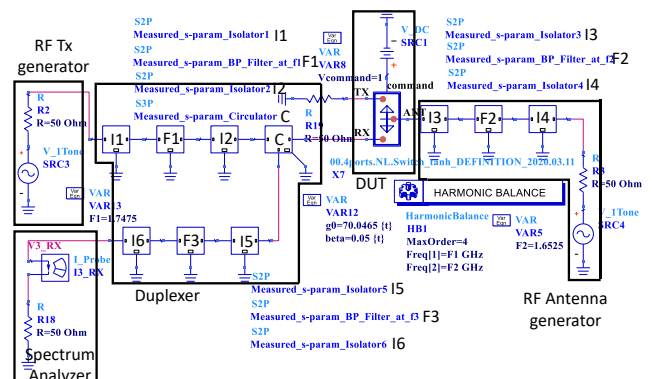


Fig. 7. ADS schematic of the virtual IMD3 test-bench

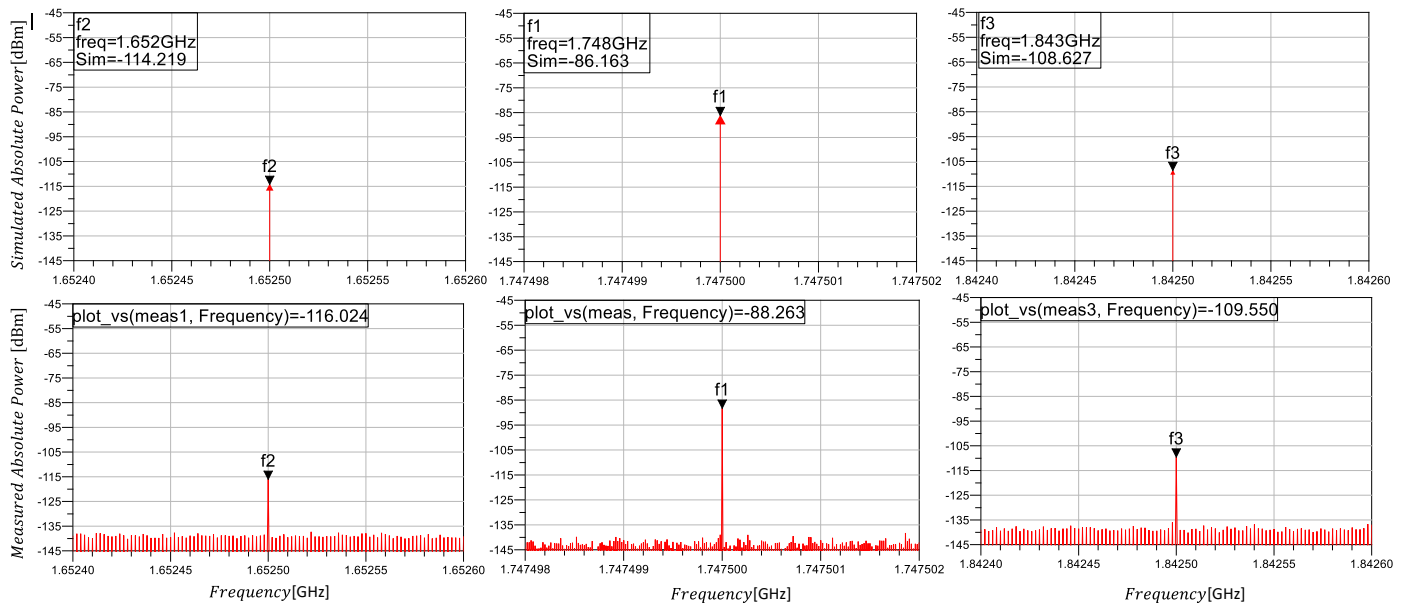


Fig. 8. Comparison between measurements results from the experimental test-bench and simulations results of the corresponding virtual test-bench at  $f_1$ ,  $f_2$  and  $f_3$ .

The virtual test-bench is composed of passive components described by their measured [S] parameters to be representative of the experimental test-bench. The RF transmission and jammer generators are replaced with Keysight ADS<sup>®</sup> software defined RF sources.

The spectrum analyzer is described with the ideal 50  $\Omega$  and the  $V_{3,Rx}$  and  $I_{3,Rx}$  probes allowing power calculation of all frequency components defined through the HB controller. A 2-tone HB simulation is then performed. Fig. 8 presents the comparison between calibrated measurements results from the experimental test-bench and simulations results of the corresponding virtual test-bench at  $f_1$ ,  $f_2$  and  $f_3$ .

The spectrum analyzer used in the experimental IMD3 test-bench allows performing a narrowband window measurement at each IMD3 frequency ( $f_1$ ,  $f_2$  and  $f_3$ ). It allows programming the resolution and video bandwidths, the attenuation and the span separately for each window measurement.

A narrowband window has been used for each frequency component ( $f_1$ ,  $f_2$  and  $f_3$ ) for measurements results from experimental IMD3 test-bench and simulations results of the corresponding virtual test-bench.

The absolute power level at the lower IMD3 frequency component ( $f_4$ ) filtered-out of the band of interest) is not presented in Fig. 8 because it is beyond the measurement sensitivity of the spectrum analyzer (beyond noise floor).

The absolute power levels of the IMD3 product  $f_3$  from measurement are in a very good agreement with the one simulated with the virtual test-bench. One can see that all parameters from the simulation matched to measurement

results. We observed less than 1 dB difference in IMD3 between simulation and measurement.

A good agreement between measurements and simulations is also observed for  $f_1$  and  $f_2$ .

To our knowledge, the development of the virtual test-bench using a 2-tone Harmonic Balance simulation associated to a schematic based on measured [S] parameters of every passive devices of the experimental test-bench and applied to a non-linear behavioral frequency defined model of a switch is described for the first time.

## V. CONCLUSION

This article presents a simple behavioral RF switch model that can be used within a virtual IMD3 test-bench. The architecture of the experimental IMD3 setup based on the use of a duplexer has been replicated and implemented in an ADS software. A 2-tone Harmonic Balance simulation has been realized. The measured and simulated results are in very good agreement in terms of IMD3 products. For the first time to our knowledge, a corresponding virtual IMD3 test-bench of an experimental IMD3 test-bench has been presented.

## REFERENCES

- [1] Tero Ranta, Juha Ellä, and Helena Pohjonen, "Antenna Switch Linearity Requirements for GSM/WCDMA Mobile Phone Front-Ends", The European Conference on Wireless Technology, Paris, France, 2005.
- [2] "Wideband SP3T RF Switch for RF diversity or RF band selection applications", Available: [www.infineon.com](http://www.infineon.com), 2016-02-03.
- [3] "3<sup>rd</sup> Generation Partnership Project; Technical Specification Group Services and System Aspects; IP Multimedia Subsystem (IMS) based Packet Switch Streaming (PSS) and Multimedia Broadcast/Multicast (MBMS) User Service; Protocols (Release)", 3GPP TS 26.237 V16.0.0 (2020-07).